Forensic Science International: Reports 2 (2020) 100114

Contents lists available at ScienceDirect

Forensic Science International: Reports

journal homepage: www.elsevier.com/locate/fsir

Forensic Anthropology

Reconstruction and physical fit analysis of fragmented skeletal remains using 3D imaging and printing

Amber J. Collings [a,b,*], Katherine Brown [b]

[a] School of Health and Life Sciences, Teesside University, Middlesbrough, TS1 3BX, United Kingdom
[b] Institute of Criminal Justice Studies, University of Portsmouth, Portsmouth, PO1 2HY, United Kingdom

ARTICLE INFO

Keywords:
Physical fit
Fragmented bone
3D printing and imaging
Burned bone reconstruction
Forensic science

ABSTRACT

Physical fit analysis (PFA) entails physically fitting fragmented evidence together to determine shared origin. PFA can be challenging to conduct with bone fragments particularly when fragile, sharp, or embedded in other materials. Three-dimensional (3D) imaging and printing techniques can circumvent these challenges. We compare two different 3D imaging techniques, micro computed tomography (μCT) and structured light scanning (SLS). By generating virtual 3D models and prints of burned human bone fragments, we test the suitability of these imaging techniques and subsequent 3D printing for PFA. We found 3D imaging and printing allowed for effective PFA without excessively handling the original fragments.

Introduction

Forensic investigation of crime scenes and other incidents requires the analysis of many different items as evidence, including human remains, some of which may be damaged or fragmented as a result of the actions during the event (such as a fire or trauma) and upon collection [1,2]. Fragmented evidence routinely undergoes physical fit analysis (PFA), a process involving manually handling and matching fragmented pieces together in order to determine whether they fit together. A positive physical fit is indicative of the two or more fragments having originated from the same object. Confirming physical fit in a forensic context can therefore draw links between scenes [3], place suspects at the scene [4], and allow for object reconstruction [5].

When conducting PFA on fragmented skeletal remains, there are instances where manual handling of the bone fragments is challenging. For example, they may pose a biological hazard [6], fragments may be extremely small [7], or the bone itself may be too fragile [2,7]. This poses a particular problem in terms of reconstruction, since current practices typically rely on manually gluing the fragments back together to allow further interpretation of the traumas [8,9]. Furthermore, the fragments (including PFA results) can be difficult to comprehensively document or present in some cases. This is particularly true for those fragments that are three dimensional (3D) and complex in nature, or are embedded in an external material (as in [3]). Consequently, two-dimensional (2D) representations of such physical fit results are not always sufficient for presentation and interpretation by experts and the courts alike [10]. Both the issues faced with handling and reconstructing the remains, and their suitable presentation, are challenges in visualisation and analysis that 3D imaging and 3D printing could help circumvent.

The use of 3D technology has become increasingly widespread within the field of forensic anthropology [11–15], and indeed the whole criminal justice system [16]. Including the application of 3D scanning and modelling to cases of dismemberment [3], in wound to weapon matching [14,17–21]), craniometrics and facial reconstruction [22–24], bite mark comparison [25], and pathology visualisation and reconstruction [3,14,26,27]. There are many different methods of generating such 3D models though, including surface scanning techniques as well as volume scanning techniques (for an overview see Refs. [28] and [16]).

While volume scanning techniques allow for high resolution images to be obtained, on the nanometre scale in some instances, they tend to be expensive, time consuming and require specialist expertise and software to operate and generate 3D models from the data. Surface scanning methods, on the other hand tend to be cheaper, and more user-friendly. Collecting surface details only, these methods generate smaller file sizes and tend to use built in software, generating 3D models of acceptable resolution. Indeed, surface scanning techniques are reliable for postmortem quantitative injury analysis [29], landmarking [30,31], and the analysis of soft tissue injuries [32].

While 3D models can be visualised virtually, they can also be 3D printed. 3D printed models can adequately represent most anatomical features [33], although some bony features such as particularly thin bone, small foramina, and acute bony projections can cause issues [33]. 3D printed models are accurate enough to produce dental models [34], to aid in maxillofacial surgery [33], and to produce custom prosthesis [35].

* Corresponding author.
E-mail address: A.Collings@tees.ac.uk (A.J. Collings).

http://doi.org/10.1016/j.fsir.2020.100114
Received 24 April 2020; Received in revised form 1 June 2020; Accepted 1 June 2020
Available online 4 June 2020

Recent work has additionally demonstrated the applicability of 3D printing for the visualisation and analysis of forensic evidence [36], demonstrating measurements accurate to within millimetres [37].

Using non-contact 3D scanning methods, 3D models of evidential fragments can therefore be generated and subsequently printed. However, to our knowledge, this approach has not yet been applied explicitly to PFA. Providing the 3D models are produced to a sufficient quality, evidential replicas, either virtual or 3D printed, offer opportunities for PFA to be conducted without having to excessively handle the original evidential fragments. Limiting the handling of fragile forensic evidence is advantageous in terms of minimising damage or contamination risks. Additionally, the use of 3D prints opens up the possibility for physical fit demonstration, and the opportunity for a jury to explore the evidence replicas. Furthermore, interaction with 3D virtual models and animations provides 360 degree visualisation in an engaging, understandable [38] and potentially impactful way, improving jury comprehension [28,39–44].

Theoretically then, 3D modelling and printing could be highly useful for visualising and conducting a physical fit of fragmented skeletal remains that are not easily handled or presented in court. In this paper, we use pieces of bone naturally fragmented through the process of burning. We compare micro Computed Tomography (μCT), a volume scanning technique, with structured light scanning (SLS) a surface scanning technique, to assess the trade-offs between the two methodologies. Subsequently, we generate 3D printed models of the bone fragments to test their potential for conducting PFA. We have two aims; 1) to determine if structured light scanning is sufficient to offer a cheaper, less labour intensive option than μCT for the 3D reconstruction of bone fragments and 2) to determine whether 3D printed replica models can be used to accurately perform PFA.

Methods

Human bone samples

The fragmented bone samples used in this study originate from a dry, archaeological human femur donated to the University of Portsmouth teaching collection. In a previous, and unrelated study, three transverse sections of the midshaft (~2−3 cm in height) were cut and burned in a Gallenkamp Muffle Furnace at 600 °C for 30−60 min. Each section of bone fragmented longitudinally, naturally, into at least two separate pieces, either during the burning process, or during cooling (See Fig. 1 for an example). For this study, the two adjoining fragments from each of the three sections were 3D imaged and printed to evaluate the techniques for their use in visualising and analysing the physical fit of burned bone fragments.

3. D imaging

The structured light scanner, an EinScan Pro + (Shining3D, China) fits on a benchtop, requires readily available computing power and comes with all the software required to produce the virtual scans, for visualisation and in preparation for printing. As this scanner relies on the reflection of white light from the surface of the object to form the image, imaging works best in a darkened room. Particularly shiny or mirrored objects can be sprayed with a very fine white powder to generate a mattified, uniform, white surface, facilitating reflection of the white light.

The ZEISS Xradia 520 Versa microCT (μCT) scanner is somewhat larger and more expensive, requiring a dedicated room and specialist technical knowledge, but is representative of the facilities available to the policing sector through academic partners. Samples require placing securely in the path of the x-ray beam within the machine; no other preparation is necessary, and it is a non-destructive process.

Structured light scanning

The EinScan Pro + (Shining3D, China) scanner was used to generate virtual models of all six bone fragments. Prior to scanning, each fragment was sprayed with Magnaflux SpotCheck SKD-S2 Developer. Each fragment was scanned separately with the use of a turntable to enable automatic mesh alignment. Two or three scans were run for each fragment, each conducted with the fragment in a different orientation. Each scan consisted of twelve 30-degree increment rotations of the turntable. The automatically aligned and merged meshes were exported from the scanner software as STL (stereolithography) files. Any minor holes in the exported files that required repair were filled post-hoc using Geomagic Design X (Version 2016.2.2., https://www.3dsystems.com/software/geomagic-design-x). The physical fragments were then cleaned using a soft brush and air puffer to remove the developer spray residue.

MicroCT scanning

Following SLS and subsequent cleaning (to remove spray powder residue), all six bone fragments were imaged in a ZEISS Xradia 520 Versa microCT (μCT) scanner at a resolution of 25.143 μm (0.4 × 80 kV 7 W).

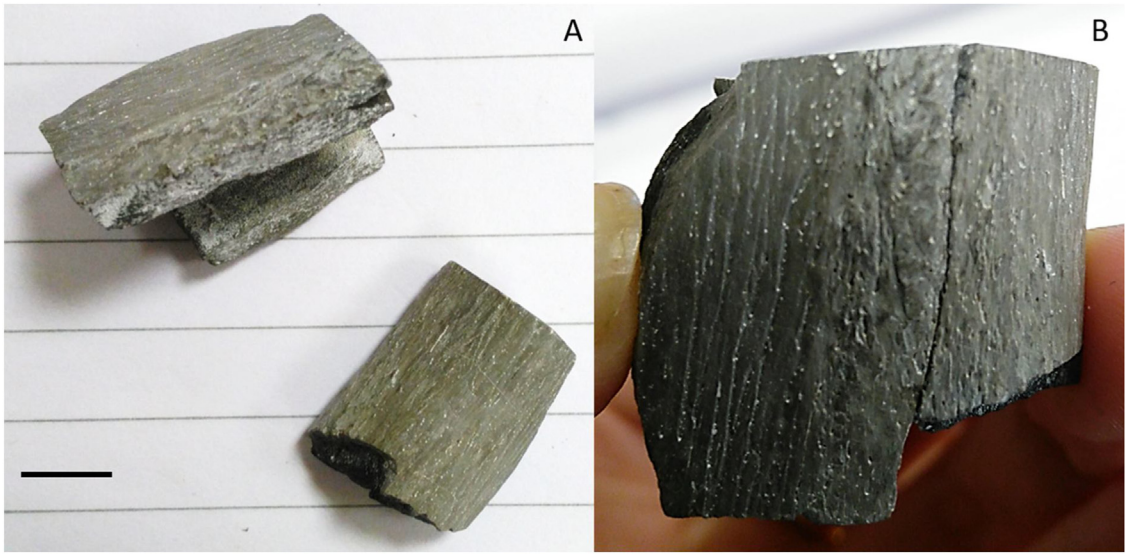

Fig. 1. Example pair of longitudinally fractured burned femur fragments (A) and a demonstration of their physical fit (B). Black scale bar in A is equal to 0.8 mm.

To ensure the samples did not move throughout scan duration, each pair of fragments were placed in a 20 mL plastic sample tube and secured in place with packaging sponge. Imaging took ~3.5 h per tube (pair of fragments).

The resulting stack of μCT image slices were cropped and resampled 1 in 4 using the Fiji plug-in for ImageJ ([45]; https://imagej.nih.gov/ij/). Amira 6.3.0 (https://www.fei.com/software/avizo3d/%C2%A0) was subsequently used to digitally segment the bone fragments. The threshold tool was used to assign voxel selections as bone material based on grayscale values. The grey scale thresholds used were chosen as the range within which all bone material was included to sufficient detail, whilst limiting the inclusion of noise or non-bone material (for all three scans this range was approximately 29300−65600HU). Any non-bone material (packing materials) included was digitally removed after material assignment using the 'Remove Islands' tool. Each bone fragment was then rendered into a 3D model using the 'Generate Surface' tool. To minimise the 'blocky' appearance of the voxels whilst maintaining sufficient surface detail for PFA, a constrained smoothing level of 3 was applied during surface generation. Each fragment surface was then exported as an STL file.

3. D print physical fit

3D print g-codes were generated using PrusaControl (Ver. 0.9.4_415_beta, http://prusacontrol.org) All fragments were printed using a Prusa i3 desktop printer, using fused filament deposition technology and PLA filament. The optimal print quality (0.15 mm) was selected and infill levels were set at 0% to create a completely hollow print. A 2 cm brim and struts from the build plate were included to help adherence to the printer bed and to prevent toppling of the model during printing. Aside from filament colour, all settings remained the same for the light scanned and μCT scanned fragments. The brim and struts were removed manually after print completion.

Physical fit analysis was conducted on the pairs of 3D printed bone fragment models. Fit was confirmed on the basis of feature matching and alignment between the two fragments as well as the haptic 'feel' of the fit. During fit analysis, positive fit could be confirmed if notable features spanning the fracture line were aligned, limited air space was present between the fragments, and fragment fit was robust to manipulation (i.e. fragments 'fix' into place as opposed to being able to move freely against each other).

Results

Table 1 provides a comparison of cost, imaging, and model processing time between the two scanning techniques. While μCT is costly and labour intensive, the available resolution is superior to that of the simpler and more affordable structured light scanner (Fig. 2).

3. D print physical fit results

All six μCT fragments and all six SLS fragments were printed together (Fig. 3A, B). Printing took ~2 h per six fragments and cost ~£3.00. The optimal printer settings (0.15 mm) preserved detail for both the μCT and SLS models well and overall produced prints that were of sufficient quality to perform PFA. Based on the fit quality criteria; feature alignment, air space between the fragments, and robustness to manipulation, confirmation of physical fit was found to be easier using the μCT prints compared with the SLS prints. For all fragment pairs, the μCT models offered a closer, and more robust fit compared with the SLS models, as well as showing endosteum surface structures in greater detail which was of value in feature matching and alignment across the fragments. The 3D prints generated using SLS scanning are therefore sufficient for visualisation and demonstration of a fit, but if wishing to conduct a robust non-destructive PFA, μCT modelling is preferable.

Discussion

In this study we used two alternative scanning techniques to image and 3D print models of burned fragmented bone. We compared techniques to assess their use in physical fit analysis (PFA). As could be expected the μCT models depicted the bone fragments in greater detail, however, both scanning methods recorded sufficient detail to allow for feature matching and fragment alignment in reconstruction and PFA; 3D printing the models retained sufficient detail to perform PFA. It should be noted, however, that the SLS technique was outperformed by μCT when it came to fit confirmation due to the superior detail afforded by the latter imaging technique.

Comparison of structured light and micro computed tomography scanning

While μCT scanning provided higher resolution models than SLS, it is a transmissive imaging technique and as such contains internal volume data. This can be advantageous in the imaging of human remains in some cases, allowing for various analyses such as subtle injury assessment [26,27] or quantitative analysis (such as in [21]). However, for PFA this level of data capture may be superfluous, since simple PFA does not require internal volume data. Furthermore, large amounts of data generate issues with secure storage space, as well as the time and cost of the approach, which requires a high level of expertise, and specialist software [16].

Surface scanning using SLS is far quicker to implement than μCT, straight forward to operate, and can be used with built in scanner software. However, the lower resolution resulted in a smoother surface where the scanner was unable to resolve finer details (as seen in Fig. 2), and the need for mattifying chalk spray prior to scanning could be problemmatic. For the bone fragments used in this study, the mattifying spray was likely required due to the slightly shiny surface of the bones

Table 1
Model, cost, imaging, and processing time for μCT and structured light scanning techniques.

	3D imaging technique	
	μCT scanning	Structured light scanning
Scanner model	Zeiss Xradia 520 Versa	EinScan Pro +
Scanner cost (at the time of purchase)	>£1 million	£5000
Pre-treatment	None required	Mattifying chalk spray
Imaging time	3.5 h per fragment pair	<30 min. per fragment
Imaging resolution	25 μm	+/- 50 μm
Imaging cost	£110 per hour	Free
Post-processing required	Segmentation	Only if holes in mesh
Post-processing time per fragment	~1 h*	~15 min
Software required	Fiji (free), Amira (~$4000)	Built-in free software, Geomagic X, or any equivalent freeware
Total time from scan to model	4 h per fragment pair	< 1 h for all fragments

* Dependant on number of slices.

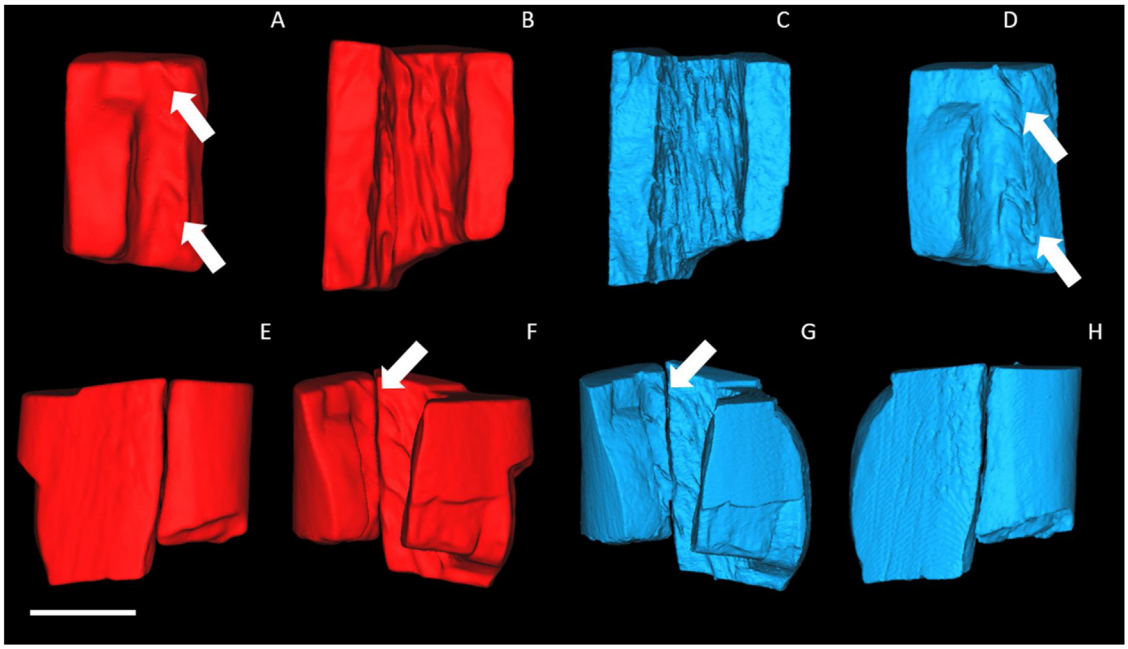

Fig. 2. Example of 3D models (A-D) aligned to demonstrate their fit (E-H). Models generated from structured light scanning are shown in red (left hand side) and those generated through μCT scanning are shown in blue (right hand side). The white arrows in A and D highlight homologous ridge details on the endosteal surface. The white arrows in F and G highlight the proximal most ridge detail use in feature matching. The white scale bar is equal to 170 mm.

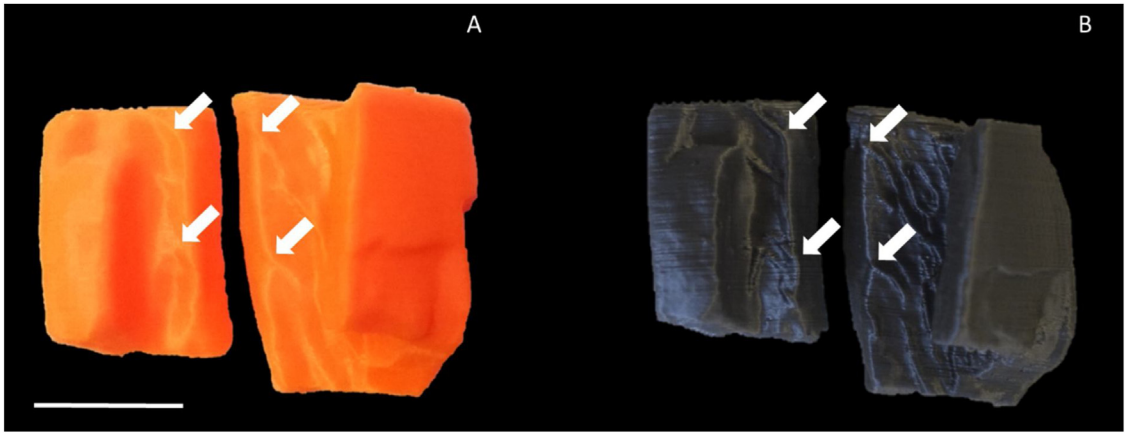

Fig. 3. The 3D printed replicas of the virtual models shown in Fig. 2. The structured light scanned model replica is printed in orange (A) and the μCT scanned model replica is printed in silver (B). The white arrows in A and B highlight the ridge details shown in Fig. 2 A and D. The white scale bar is equal to 170 mm.

after burning and the darkening of their colour. By virtue of using light pattern deformation, black and/or shiny items are particularly challenging to image using the SLS technique [46]. The mattifying spray itself is a chalk and alcohol mix, that it can be dusted off once dry, if required. While this is likely to work well for some larger and smoother bone surfaces, removing all residue was challenging and time consuming with the burned bone fragments used here because of their fragility and micro-scale features. Photogrammetry could be used as an alternative surface imaging technique but without further research into the resolution we cannot be sure that enough fine detail would be captured using that method. For those reasons, as well as contamination risks, it is not recommended that fragile bone fragments of particular forensic relevance be sprayed, limiting the ability of SLS to be used for reconstruction in certain cases.

Use of 3D printing for physical fit analysis

The work presented here demonstrates that fused filament deposition (FFD; also referred to as fused deposition modelling or FDM) 3D printing retains the appropriate detail for PFA of replica evidence fragments despite its lower resolution compared with the imaging techniques. The models were printed at a resolution of 0.15 mm (the optimal setting for the printer model) which is approximately 3–6 times lower than either of the imaging techniques used. Nonetheless, both SLS and μCT techniques worked well, producing appropriate prints. The SLS prints were more suitable for demonstration as opposed to analysis, however. The preferable model quality was obtained using μCT imaging.

The FFD method is a common form of additive material printing. It works by exuding material and building up the 3D model on to the print bed in a series of layers. Depending on the geometry of the 3D model being printed, one of the drawbacks of using FFD printers is the requirement for support structures which prevent movement or toppling of the print during the printing process. Such support structures can be difficult to remove without print damage (especially around finer details or overhanging sections) and may leave rough surfaces on the print after removal [37]. Research by Carew et al. [37] suggests selective laser sintering is the most metrically accurate printing methodology and recommends its use in favour of FFD. Since

selective laser sintering printing builds the 3D model from a reservoir of nylon powder, with a laser tracing and hardening the powder layer by layer, the resulting 3D model is encased in the build material, negating the requirement for support structures and increasing surface quality [37].

Unsurprisingly though, while selective laser sintering may be recommended as the 'gold standard' for 3D printing of evidence, it is a far more costly option. While selective laser sintering printers cost between $5000 and $175,000 (~£3800–£135,000) [47], the FFD Prusa model used in the current study is a fraction of that price (> $1300/£1000). Cheaper desktop options are discouraged, due to a lack of accuracy [48], yet, as demonstrated in Carew et al. [37] and indeed the current research, desktop FFD can produce accurate prints. Moreover, the 3D printed bone fragments of the current paper were arranged on the print bed to minimise the requirement for support structures and were orientated vertically to minimise print artefacts and detrimental effects on surface quality, especially along the fracture surfaces. We were therefore able to produce high quality prints with very little support and a brim that could be easily removed without damage. It is therefore worth noting that if opting to use FFD printing methods that the potential for artefacts and quality issues can be minimised by consideration of the position and orientation of the model on the print bed. In summary, while selective laser sintering is recommended, desktop FFD methods as used here offer an excellent and affordable alternative.

Conducting PFA analyses on the 3D printed bone fragments relied on both the haptic 'feel' of the fit and the use of feature matching across the fracture site (See Figs. 2 and 3). Feature matching was possible with the 3D print replicas from both imaging techniques, however as previously mentioned the lower resolution of SLS scanning did mean the ridge features were subtler than in the μCT prints. The fracture patterns observed in the bone fragments of this study could be described as simple clean fractures. The bones naturally fragmented during the cooling process post-burning, and therefore do not represent complex or traumatic fractures such as seen in Baier et al. [3] where traumatic dismemberment occurred. Without a direct comparison, we cannot be certain whether 3D print reconstruction would be either more or less challenging with a simple versus complex fracture. The 'natural' fractures seen here are likely to fit together very well since there was limited opportunity for small slithers of bone to be lost or irreparably damaged, compared with a traumatic and complex fracture where elements of crushing and shear forces may prevent perfect reconstruction. That being said, the simple fractures seen here are smooth and lack such interdigitating (or zig-zagged) elements seen in the fragments from Baier et al. [3]. Traumatic fractures are perhaps more likely to be unique in their morphology, while the interdigitation of fragment edges would allow for reconstructions that are robust to manipulation. We encourage future research into the effectiveness of 3D print reconstructions for a range of fracture types and complexities.

The application of 3D imaging and printing for PFA has many advantages compared with traditional methods. While the samples used here represent a relatively simple and clean natural fracture, using analyses similar to that applied to fossil human fragmented remains ([49], for example), virtual reconstruction of highly fragmented, fragile, and potentially embedded remains offers an opportunity to generate full reconstructions without compromising the original bone fragments. This is equally applicable to evidential remains that pose biological or mechanical hazard [3]; 3D printing further provides means to manually manipulate those remains safely, while preserving their integrity, an important element for forensic osteological analyses. Furthermore, 3D prints from particularly small fragments or bones with micro-scale details can be isometrically scaled up, generating 3D replicas to visualise fit and perform PFA on items that previously would have been extremely challenging. On the other hand, larger, heavy elements can be isometrically scaled down and replicated into lightweight manageable models which are far easier to manipulate and transport.

Summary

In summary, while SLS certainly demonstrated potential, it was outperformed by μCT in terms of imaging small burned bone fragments. The requirement for mattifying spray and reduced resolution compared with μCT meant it was only an acceptable alternative for visualisation purposes and not fit confirmation. Fused filament deposition (FFD) 3D printing proved to be an accurate and useful method for creating physical replicas of the bone fragments to perform physical fit analysis (PFA) and bone fragment reconstruction. We therefore recommend μCT imaging paired with FFD 3D printing as an excellent option for non-destructive physical fit confirmation when working with small fragments and burned bone. Overall, the techniques demonstrated here are of value in forensic investigation and evidence presentation within the courtroom.

Funding

This research was supported by internal funding by the Institute of Criminal Justice Studies, University of Portsmouth.

Declaration of Competing Interest

Authors report no conflicts of interest.

CRediT authorship contribution statement

Amber J. Collings: Conceptualization, Methodology, Resources, Investigation, Writing - review & editing, Visualization. **Katherine Brown:** Methodology, Resources, Writing - review & editing, Funding acquisition.

Acknowledgements

Authors would like to thank Alex Kao for his assistance conducting the μCT scanning, Will Keeble for his assistance conducting structured light scanning, and the University of Portsmouth for allowing access to the human bone for research purposes. Additionally, thanks goes to Dr James Charles, Dr Ed Rollason, and Professor Tim Thompson for their valuable comments on draft versions of the manuscript. Finally, many thanks goes to the editior and to the reviewer for their time and constructive feedback.

References

[1] R.C. Shaler, Crime Scene Forensics: A Scientific Method Approach, CRC Press, Taylor & Francis Group, Boca Raton, USA, 2011.
[2] D.A. Komar, S. Davy-Jow, S.J. Decker, The use of a 3-D laser scanner to document ephemeral evidence at crime scenes and postmortem examinations, J. Forensic Sci. 57 (2012) 188–191.
[3] W. Baier, D.G. Norman, J.M. Warnett, M. Payne, N.P. Harrison, N.C.A. Hunt, B.A. Burnett, M.A. Williams, Novel application of three-dimensional technologies in a case of dismemberment, Forensic Sci. Int. 270 (2017) 139–145.
[4] M.J. Bradley, R.L. Keagy, P.C. Lowe, M.P. Rickenbach, D.M. Wright, M.A. LeBeau, A validation study for duct tape end matches, J. Forensic Sci. 51 (2006) 504–508.
[5] A.M. Christiansen, A.D. Sylvester, Physical matches of bone, shell and tooth fragments: a validation study, J. Forensic Sci. 53 (2008) 694–698.
[6] J.T. Fish, R.N. Stout, E. Wallace, Practical Crime Scene Investigations for Hot Zones, CRC Press, USA, 2010.
[7] R.W. Jackson, J.M. Jackson, Forensic Science, 4th ed., Pearson Education Limited, Harlow, UK, 2017.
[8] G. Grévin, P. Bailet, G. Quatrehomme, A. Ollier, Anatomical reconstruction of fragments of burned human bones: a necessary means for forensic identification, Forensic Sci. Int. 96 (1998) 129–134.
[9] S. Blau, How traumatic: a review of the role of the forensic anthropologist in the examination and interpretation of skeletal trauma, Aust. J. Forensic Sci. 49 (2017) 261–280.
[10] N.D. Tung, J. Barr, D.J. Sheppard, D.A. Elliot, L.S. Tottey, K.A.J. Walsh, Spherical photography and virtual tours for presenting crime scenes and forensic evidence in New Zealand courtrooms, J. Forensic Sci. 60 (2015) 753–758.
[11] C. Robinson, R. Eisma, B. Morgan, A. Jeffery, E.A.M. Graham, S. Black, G.N. Rutty, Anthropological measurement of lower limb and foot bones using multi-detector computed tomography, J. Forensic Sci. 53 (2008) 1289–1295.

[12] S.J. Decker, S.L. Davy-Jow, J.M. Ford, D.R. Hibelink, Virtual determination of sex: metric and nonmetric traits of the adult pelvis from 3D computed tomography models, J. Forensic Sci. 56 (2011) 1107–1114.
[13] W.D. Zech, G. Hatch, L. Siegenthaler, M.J. Thali, S. Lösch, Sex determination from os sacrum by postmortem CT, Forensic Sci. Int. 221 (2012) 39–43.
[14] S. Grabherr, P. Baumann, C. Minoiu, S. Fahrni, P. Mangin, Post-mortem imaging in forensic investigations: current utility, limitations, and ongoing developments, Res. Rep. Forensic Med. Sci. 6 (2016) 25–37.
[15] R.M. Carew, M.D. Viner, G. Conlogue, N. Márquez-Grant, S. Beckett, Accuracy of computed radiography in osteometry: a comparison of digital imaging techniques and the effect of magnification, J. Forensic Radiol. Imaging 19 (100348) (2019) .
[16] R.M. Carew, D. Errickson, Imaging in forensic science: five years on, J. Forensic Radiol. Imaging 16 (2019) 24–33.
[17] M.J. Thali, M. Braun, W. Brueschweiler, R. Dirnhofer, 'Morphological imprint': determination of the injury-causing weapon from the wound morphology using forensic 3D/CAD-supported photogrammetry, Forensic Sci. Int. 132 (2003) 177–181.
[18] M.J. Thali, M. Braun, R. Dirnhofer, Optical 3D surface digitizing in forensic medicine: 3D documentation of skin and bone injuries, Forensic Sci. Int. 137 (2003) 203–208.
[19] B.S. De Bakker, V. Soerdjbalie-Maikoe, H.M. De Bakker, The use of 3D-CT in weapon caused impression fractures of the skull, from a forensic radiological point of view, J. Forensic Radiol. Imaging 1 (2013) 176–179.
[20] K. Woźniak, E. Rzepecka-Woźniak, A. Moskała, J. Pohl, K. Latacz, B. Dybała, Weapon identification using antemortem computed tomography with virtual 3D and rapid prototype modeling—a report in a case of blunt force head injury, Forensic Sci. Int. 222 (2012) e29–e32.
[21] D. Norman, D. Watson, B. Burnett, P. Fenne, M. Williams, The cutting edge — micro-CT for quantitative toolmark analysis of sharp force trauma to bone, Forensic Sci. Int. 283 (2018) 156–172.
[22] S. Park, H. Yu, K. Kim, K. Lee, H. Baik, A proposal for a new analysis of craniofacial morphology by 3-dimensional computed tomography, Am. J. Orthod. Dentofacial Orthop. 129 (2006) e23–e34.
[23] S. Benazzi, P. Bertelli, B. Lippi, R. Caudana, G. Gruppioni, F. Mallegni, Virtual anthropology and forensic arts: the facial reconstruction of Ferrante Gonzaga, J. Archaeolog. Sci. 37 (2010) 1572–1578.
[24] Z. Fourie, J. Damstra, P.O. Gerrits, Y. Ren, Evaluation of anthropometric accuracy and reliability using different three-dimensional scanning systems, Forensic Sci. Int. 207 (2011) 127–134.
[25] S. Naether, U. Buck, L. Campana, R. Breitbeck, M. Thali, The examination and identification of bite marks in foods using 3D scanning and 3D comparison methods, Int. J. Legal Med. 126 (2012) 89–95.
[26] G. Ampanozi, T.D. Ruder, U. Preiss, K. Aschenbroich, T. Germerott, L. Filograna, M.J. Thali, Virtopsy: CT and MR imaging of a fatal head injury caused by a hatchet: a case report, Legal Med. 12 (2010) 238–241.
[27] W. Baier, C. Mangham, J.M. Warnett, M. Payne, M. Painter, M.A. Williams, Using histology to evaluate micro-CT findings of trauma in three post-mortem samples — first steps towards method validation, Forensic Sci. Int. 297 (2019) 27–34.
[28] D. Errickson, T.J.U. Thompson, B.W.J. Rankin, The application of 3D visualization of osteological trauma for the courtroom: a critical review, J. Forensic Radiol. Imaging 2 (2014) 132–137.
[29] S.A. Blackwell, R.V. Taylor, I. Gordon, C.L. Ogleby, T. Tanijiri, M. Yoshino, M.R. Donald, J.G. Clement, 3-D imaging and quantitative comparison of human dentitions and simulated bite marks, Int. J. Legal Med. 121 (2007) 9–17.
[30] S.C. Aung, R.C.K. Ngim, S.T. Lee, Evaluation of the laser scanner as a surface measuring tool and its accuracy compared with direct facial anthropometric measurements, Br. J. Plast. Surg. 48 (1995) 551–558.
[31] S.B. Sholts, S.K.T.S. Wärmländer, L.M. Flores, K.W.P. Miller, P.L. Walker, Variation in the measurement of cranial volume and surface area using 3D laser scanning technology, J. Forensic Sci. 55 (2010) 871–876.
[32] A. Shamata, T. Thompson, Determining the effectiveness of noncontact three-dimensional surface scanning for the assessment of Open injuries, J. Forensic Sci. 65 (2019) 627–635.
[33] D.M. Silva, M.G. de Oliveira, E. Meurer, I. Meurer, J.V.L. da Silva, A. Santa-Bárbara, Dimensional error in selective laser sintering and 3D-printing of models for craniomaxillary anatomy reconstruction, J. of Cranio-Maxillofacial Surg. 38 (2008) 443–449.
[34] A. Hazeveld, J.J.R. Huddleston Slater, Y. Ren, Accuracy and reproducibility of dental replica models reconstructed by different rapid prototyping techniques, Am. J. Orthod. Dentofacial Orthop. 145 (2014) 108–115.
[35] A. Marro, T. Bandukwala, W. Mak, Three-dimensional printing and medical imaging: a review of the methods and applications, Curr. Probl. Diagn. Radiol. 45 (2016) 2–9.
[36] J. Edwards, T. Rogers, The accuracy and applicability of 3D modeling and printing blunt force cranial injuries, J. Forensic Sci. 63 (2017) 683–691.
[37] R.M. Carew, R.M. Morgan, C. Rando, A preliminary investigation into the accuracy of 3D modeling and 3D printing in forensic anthropology evidence reconstruction, J. Forensic Sci. 64 (2018) 342–352.
[38] W.F. Gotsmy, L.C. Ebert, M. Bolliger, G.M. Hatch, T. Ketterer, M.J. Thali, T.D. Ruder, A picture is worth a thousand words – the utility of 3D visualization illustrated by a case of survived pancreatic transection, Legal Med. 13 (2011) 95–97.
[39] L.C. Ebert, M.J. Thali, S. Ross, Getting in touch—3D printing in forensic imaging, Forensic Sci. Int. 211 (2011) e1–e6.
[40] M. Grassberger, A. Gehl, K. Püschel, E.E. Turk, 3D reconstruction of emergency cranial computed tomography scans as a tool in clinical forensic radiology after survived blunt head trauma—Report of two cases, Forensic Sci. Int. 207 (2011) e19–e23.
[41] W. Baier, J.M. Warnett, M.P. Payne, M.A. Williams, Introducing 3D printed models as demonstrative evidence at criminal trials, J. Forensic Sci. 63 (2017) 1298–1302.
[42] C. Villa, K.B. Olsen, S.H. Hansen, Virtual animation of victim-specific 3D models obtained from CT scans for forensic reconstructions: living and dead subjects, Forensic Sci. Int. 278 (2017) e27–e33.
[43] S. Blau, E. Phillips, C. O'Donnell, G. Markowsky, Evaluating the impact of different formats in the presentation of trauma evidence in court: a pilot study, Aust. J. Forensic Sci. 51 (2018) 695–704.
[44] D. Errickson, H. Fawcett, T.J.U. Thomposon, A. Campell, The effect of different imaging techniques for the visualisation of evidence in court on jury comprehension, Int. J. Legal Med. (2019) [Epub ahead of print].
[45] J. Schindelin, I. Arganda-Carreras, E. Frise, et al., Fiji: an open-source platform for biological-image analysis, Nat. Methods 9 (2012) 676–682.
[46] D. Errickson, I. Grueso, S.J. Griffith, J.M. Setchell, T.J.U. Thompson, C.E.L. Thompson, R.L. Gowland, Towards a Best practice for the use of active non-contact surface scanning to record human skeletal remains from archaeological contexts, International Journal of Osteoarchaeology 27 (2017) 650–661.
[47] T. Koslow, SLS 3D Printer Buyer'S Guide. All3DP.Pro, (2019) https://all3dp.com/1/best-sls-3d-printer-desktop-industrial/.
[48] T. Hodgdon, R. Danrad, M.J. Patel, S.E. Smith, M.L. Richardson, D.H. Ballard, et al., Logistics of three-dimensional printing: primer for radiologists, Acad. Radiol. 25 (2018) 40–51.
[49] R.M. Godinho, P. O'Higgins, Virtual reconstruction of cranial remains: the *H. Heidelbergensis*, Kabwe 1 fossil, Human Remains - Another Dimension: The Application of 3D Imaging in Funerary Context, Elsevier, London, UK, 2017, pp. 135–147.